

DISK GALAXY ROTATION CURVES IN TRIAXIAL CDM HALOS

ERIC HAYASHI,¹ JULIO F. NAVARRO,^{1,2} ADRIAN JENKINS,³ CARLOS S. FRENK,³ CHRIS POWER,³
SIMON D.M. WHITE,⁴ VOLKER SPRINGEL,⁴ JOACHIM STADEL,⁵
THOMAS QUINN,⁶ AND JAMES WADSLEY⁷

Draft version March 20, 2022

ABSTRACT

We use N-body hydrodynamical simulations to study the structure of disks in triaxial potentials resembling CDM halos. Our analysis focuses on the accuracy of the dark mass distribution inferred from rotation curves derived from simulated long-slit spectra. We consider a massless disk embedded in a halo with axis ratios of 0.5:0.6:1.0 and with its rotation axis aligned with the minor axis of the halo. Closed orbits for the gaseous particles deviate from coplanar circular symmetry, resulting in a variety of long-slit rotation curve shapes, depending on the orientation of the disk relative to the line of sight. Rotation curves may thus differ significantly from the spherically-averaged circular velocity profile of the dark matter halo. “Solid-body” rotation curves—typically interpreted as a signature of a constant density core in the dark matter distribution—are obtained about 25% of the time for random orientations although the dark matter follows the cuspy density profile proposed by Navarro, Frenk & White (NFW). We conclude that the discrepancies reported between the shape of the rotation curve of low surface brightness galaxies and the structure of CDM halos may be resolved once the complex effects of halo triaxiality on the dynamics of the gas component is properly taken into account.

Subject headings: cosmology: dark matter – galaxies: formation – galaxies: kinematics and dynamics

1. INTRODUCTION

It is commonly believed that the inner regions of low surface brightness (LSB) galaxies are ideal probes of the inner structure of dark matter halos. Given the small contribution of the baryonic component to the mass budget in these galaxies, dynamical tracers of the potential such as rotation curves are expected to cleanly trace the dark matter distribution. This provides important astrophysical clues to the nature of dark matter, since the spatial distribution of dark material in these highly non-linear regions is expected to be quite sensitive to the physical properties of the dark matter.

LSB rotation curves can thus be contrasted directly with theoretical predictions of the inner structure of halos, and there is now an extensive body of work in the literature that reports substantial disagreement between the shape of LSB rotation curves and that of circular velocity curves of simulated cold dark matter (CDM) halos (see, e.g., Flores & Primack 1994; Moore 1994; McGaugh & de Blok 1998; de Blok et al. 2001). Some of these rotation curves are fit better by circular velocity curves arising from density profiles with a constant density “core” rather than by the “cuspy” density profiles commonly used to fit the structure of CDM halos

(Navarro, Frenk & White 1996, 1997, hereafter NFW). This discrepancy adds to a growing list of concerns regarding the consistency of CDM with observational constraints on the scale of individual galaxies (see, e.g., Sellwood & Kosowsky 2001) that has prompted calls for a radical revision of the CDM paradigm on small scales (see, e.g., Spergel & Steinhardt 2000).

Before accepting the need for radical modifications to CDM it is important to note a number of caveats that apply to the LSB rotation curve problem. For instance, many of the early rotation curves where the disagreement was noted were significantly affected by beam smearing in the HI data (Swaters et al. 2000). The observational situation has now improved substantially thanks to higher-resolution rotation curves obtained from long-slit H α observations (see, e.g., de Blok & Bosma 2002; Swaters et al. 2003). We shall restrict our analysis to these newer datasets in what follows.

We also note that, strictly speaking, the observational disagreement is with the fitting formulae used to parameterize the structure of simulated CDM halos (usually the profile proposed by NFW), rather than with the structure of simulated halos themselves. Although the fitting formulae provide a simple and reasonably accurate description of the mass profile of CDM halos, the radial range over which they have been validated often does not coincide with the scales where the disagreement has been identified.

Furthermore, small but significant deviations between the NFW profile and simulated halos have been reported as the mass and spatial resolution of the simulations has increased (Moore et al. 1998; Ghigna et al. 2000; Fukushige & Makino 1997, 2001). Although there is no broad consensus yet regarding how these deviations may affect the comparison with observed rotation curves (see, e.g., Power et al. 2003; Hayashi et al. 2003; Navarro et al. 2004), the fact that the deviations worsen

¹ Department of Physics and Astronomy, University of Victoria, Victoria, BC V8P 1A1, Canada

² Fellow of CIAR and of the J.S.Guggenheim Memorial Foundation

³ Institute for Computational Cosmology, Department of Physics, University of Durham, South Road, Durham DH1 3LE, United Kingdom

⁴ Max Planck Institute for Astrophysics, Karl-Schwarzschild Strasse 1, Garching, Munich, D-85740, Germany

⁵ Institute for Theoretical Physics, University of Zurich, Winterthurerstrasse 190, Zurich CH-8057, Switzerland

⁶ Department of Astronomy, University of Washington, Seattle, WA 98195, USA

⁷ Department of Physics and Astronomy, McMaster University, Hamilton, ON L8S 4M1, Canada

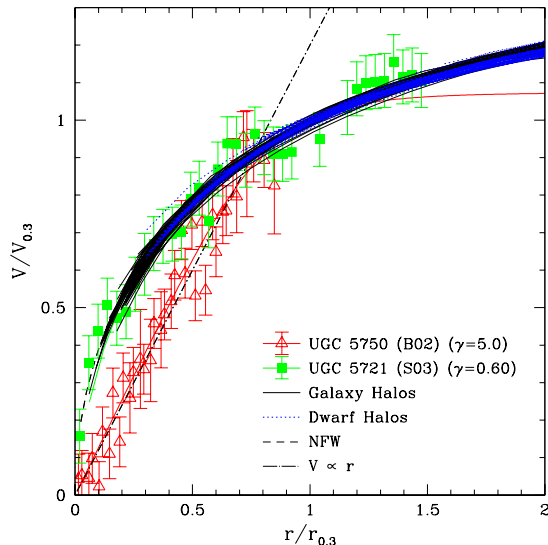


FIG. 1.— Rotation curves of two LSB galaxies from the samples of de Blok & Bosma (2002, B02) and Swaters et al. (2003, S03), chosen to illustrate their various shapes, as measured by the parameter γ from fits with the Courteau (1997) fitting formula. Rotation curves have been scaled to the radius $r_{0.3}$ and corresponding velocity $V_{0.3}$ (see text for details). Fits with large γ values are characterized by a linear rise in velocity with radius followed by a sharp transition to the flat part of the curve. The NFW profile (dashed line) and the V_c profiles of simulated dwarf- (dotted lines) and galaxy-sized halos (solid lines) match reasonably well systems with $\gamma \lesssim 1$ but cannot account for those with $\gamma \gg 1$.

towards the centre advise against using extrapolations of simple fitting formulae such as the NFW profile to assess consistency with observation.

Finally, it must be emphasized that the “cusp vs. core” problem arises when comparing rotation speeds of LSB disks to spherically-averaged circular velocities of dark matter halos. Given that CDM halos are expected to be significantly non-spherical (Davis et al. 1985; Frenk et al. 1988; Jing et al. 1995; Jing & Suto 2002), some differences between the two are to be expected. It is therefore important to use the full 3D structure of CDM halos to make predictions regarding the rotation curves of gaseous disks that may be compared directly to observation.

We address the latter issue in this *Letter*, by exploring numerically the closed orbits of gaseous particles within the potential of an idealized triaxial CDM halo. We embed a massless, isothermal gaseous disk within a cuspy dark matter halo and evolve it until equilibrium is reached.

We focus our analysis on the *shape* of the rotation curves inferred for the disk from simulated long-slit observations of the velocity field; on deviations from the spherically-averaged circular velocity curve; and on the possibility that such deviations might account for the discrepancy between LSB rotation curves and NFW profile fits to CDM halos.

2. LSB ROTATION CURVES

Figure 1 illustrates the disagreement alluded to above. This figure shows the H α rotation curves of two LSB galaxies (points with error bars) selected from the sam-

ple of de Blok & Bosma (2002, B02) and Swaters et al. (2003, S03). The data points have been fitted using a simple formula, $V_{\text{rot}}(r) = V_0(1+(r/r_t)^{-\gamma})^{-1/\gamma}$ (Courteau 1997). Here V_0 and r_t are dimensional scaling parameters, whereas γ is a dimensionless parameter that characterizes the *shape* of the rotation curve. This three-parameter formula provides excellent fits to both LSBs, as illustrated by the quality of the (solid line) fits shown in Figure 1.

In order to emphasize discrepancies in shape, the rotation curves in Figure 1 have been scaled to the radius, $r_{0.3}$, and velocity, $V_{0.3}$, where the logarithmic slope of the curve is $d \log V_{\text{rot}}/d \log r = 0.3$. The two galaxies shown in Figure 1 have different values of γ , and have been chosen to illustrate the extreme cases in the B02 and S03 datasets. Roughly one third of their LSBs have $\gamma \lesssim 1$, having rotation curves with shapes similar to UGC 5721 ($\gamma = 0.6$).

The dashed line in Figure 1 shows the V_c profile of an NFW halo, which is fixed in these scaled units. Galaxies with $\gamma \lesssim 1$ are consistent with NFW, whereas those with $\gamma \gg 1$ are clearly inconsistent. Figure 1 also shows the spherically-averaged V_c profiles of all galaxy-sized halos presented in Hayashi et al. (2003) and Navarro et al. (2004), scaled to $r_{0.3}$ and $V_{0.3}$. We find that the shapes of the dark halo V_c curves are in fact quite similar to NFW. In terms of the γ parameter, most halos (about 95%) have $\gamma \lesssim 1$, which implies that LSBs with $\gamma \gg 1$ are quite difficult to reconcile with the V_c profiles of simulated CDM halos.

On further examination, however, Hayashi et al. (2003) note that most rotation curves that have best fit values of $\gamma > 1$ also have acceptable fits with $\gamma \leq 1$. As a result, only a small minority of LSBs (about 10%) are robustly inconsistent with CDM halo V_c profiles. Most of these curves are characterized by a linear rise in velocity with radius and have best fit values of $\gamma \gtrsim 5$. One such example, UGC 5750, is shown in Figure 1, along with a dot-dashed line that illustrates the $V \propto r$ dependence expected in the presence of a constant density core.

Does this result rule out the presence of a cusp in the dark matter density profile in such galaxies? As noted in § 1, before concluding so one must take into account possible systematic differences between rotation speed and circular velocity in gaseous disks embedded within realistic, triaxial halos. This is a complex issue that involves a number of parameters, such as the degree of triaxiality, the role of the disk’s self-gravity, size, and orientation, as well as the possibility of transient deviations from equilibrium.

To keep matters simple, we have decided to address this issue by evolving a massless gaseous disk at the centre of a fixed triaxial halo. We use the N-body/hydrodynamical code GASOLINE, developed by J.Wadsley, J.Stadel, and T.Quinn (Wadsley et al. 2004). GASOLINE combines a tree-based Poisson solver for gravitational interactions with the Smooth Particle Hydrodynamics (SPH) technique. The dark matter halo is modelled with a particle realization of an NFW mass profile; the mass, virial radius and concentration of the halo are normalized to $M_{200} = 10^{11} M_\odot/h$, $r_{200} = 75 h^{-1} \text{kpc}$ and $c = 12$, respectively. In order to reduce computational expense, the halo is truncated at an outermost radius,

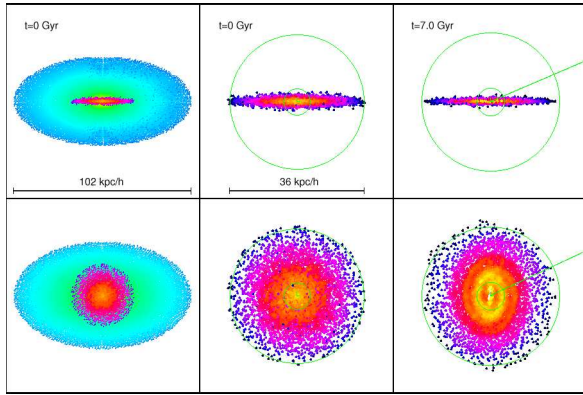


FIG. 2.— Evolution of a massless gaseous disk in the 3D potential of an idealized CDM halo. Upper (lower) panel shows edge-on (face-on) projections of the disk. Left panels show halo and disk particles at the initial time, color-coded by local dark matter and gas density, respectively. Middle and right panels show disk particles only at initial time and after 7.0 Gyr, respectively. Inner and outer circles have radii equal to the exponential scale length of the disk, r_d , and the outermost radius of the disk, r_{outer} , at $t = 0$, respectively. The straight lines in the right panels show projections of the line-of-sight used to generate the rotation curve in the lower right panel of Figure 3. Triaxiality in the halo mass distribution leads to significant evolution in the structure of the disk and to strong deviations from circular symmetry.

$r_{\text{trunc}} = 37.5 h^{-1}\text{kpc}$ and the number of particles within this radius is set to 1.7×10^5 . The halo is made triaxial by multiplying the x -, y -, and z -coordinates of the halo particles by factors of 1.36, 0.82, and 0.68, respectively, so that the spherically-averaged mass profile remains unchanged, but the axis ratios of the halo are 0.5:0.6:1.0. We note that such halo shapes (roughly prolate with elongation 2:1) are among the most common ones found in cosmological simulations (see, e.g., Jing & Suto 2002). The gravitational potential is derived directly from the dark matter particle positions and is assumed to remain constant in time.

An exponential disk consisting of 10^4 massless gas particles is placed at the centre of the halo, in the plane of the major and intermediate axes of the halo (see Figure 2). The exponential scale length of the disk is $r_d = 3.6 h^{-1}\text{kpc}$, and its outermost radius is $r_{\text{outer}} = 18.0 h^{-1}\text{kpc}$. The vertical distribution of the disk material is given by $\rho(z) \propto \text{sech}^2(z/z_0)$, with $z_0 = 0.6 h^{-1}\text{kpc}$, and the disk is truncated at $z_{\text{max}} = 3.0 h^{-1}\text{kpc}$. The gas is given a temperature $T = 100 K$, well below the virial temperature of the halo, $T_{\text{vir}} \simeq 2 \times 10^5 K$, and is assumed to remain isothermal during the evolution. Pressure forces are thus unimportant for the dynamics of the gas, and the hydrodynamical treatment simply forces the gas to provide a massless tracer of the closed orbits within the halo potential.

The disk particles are initially given tangential velocities consistent with the spherically-averaged circular velocity profile of the triaxial dark matter halo. As a result the gaseous disk is not initially in equilibrium and it evolves rapidly to a configuration characterized by departures from circular symmetry (the disk becomes elliptical, see Figure 2). The effect of such departures from circular symmetry on rotation curves derived from long-slit spectra is complex, as illustrated in Figure 3. This figure compares the rotation speed of the gas, as inferred from

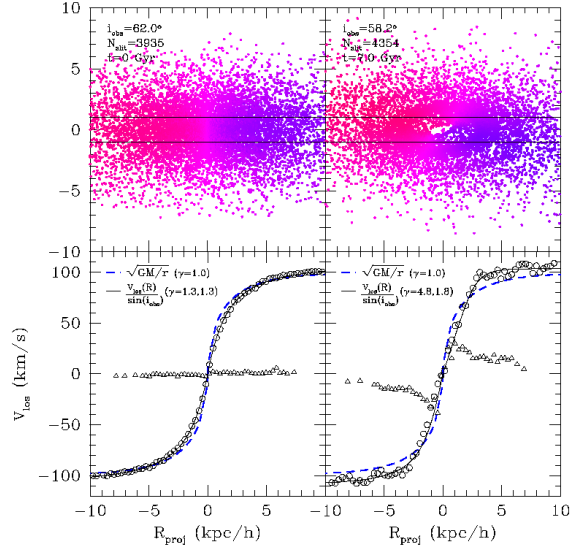


FIG. 3.— *Upper panels*: Projected positions of the disk particles after the disk has been inclined by 67° relative to the initial plane of the disk. Disk particles are color-coded by line-of-sight velocity. Solid horizontal lines indicate the position of a $2 h^{-1}\text{kpc}$ wide slit oriented along the photometric major axis of the projected disk. *Lower panels*: Rotation curve as inferred from simulated long-slit radial velocity data with slit placed across the major axis (open circles) and minor axis (open triangles) of the disk. The major axis rotation curve agrees well initially ($t = 0$) with the V_c profile of the halo (dotted curves) but significant deviations and misalignment of the kinematic and photometric major axes result from the evolution of the disk in the triaxial potential of the halo.

line-of-sight velocities measured on a slit placed along the photometric major axis of the disk determined from the projected particle distribution. The disk is inclined by 67° , and velocities are corrected by the sine of the inclination angle, i_{obs} , as derived from the aspect ratio of the isodensity contours of the gas.¹

The left panels in Figure 3 show that initially, when the disk is circularly symmetric by construction, the disk inclination is recovered reasonably accurately and the rotation speed inferred from line-of-sight velocities (open circles) agree well with the spherically-averaged circular velocity (dashed line). Fitting the halo V_c profile out to $r_{\text{outer}} = 18 h^{-1}\text{kpc}$ using the (r_t, γ, V_0) formula results in best fit values of $\gamma = 1$, whereas the initial disk rotation curve is best fit by $\gamma = 1.3$.

At later times the evolution of the disk leads to poorer estimates of the inclination as well as to significant deviations between inferred rotation speed and circular velocity. The *shape* of the rotation curve, in particular, is affected, as shown in the right-hand panels in Figure 3. On some projections, rotation curves appear to rise and turn abruptly, and they would be (erroneously) taken to imply the existence of a constant-density core in simple models that assume spherical symmetry. Fits to the disk rotation curves using the (r_t, γ, V_0) formula introduced above often have $\gamma \gg 1$, consistent with galaxies where NFW profiles provide a particularly poor fit to the rotation curve data. The open triangles in the lower panels

¹ This is inferred to be $\simeq 58^\circ$ because the disk is not circularly symmetric.

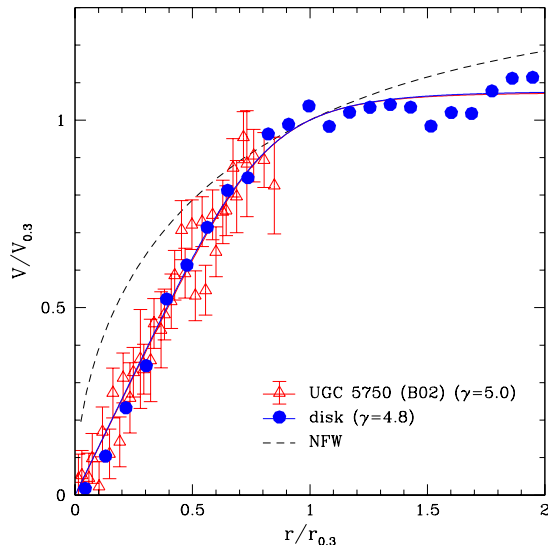


FIG. 4.— Systematic deviations from circular velocity induced by the triaxiality of the halo lead to rotation curve shapes in better agreement with LSBs with high γ . Open circles correspond to rotation curves inferred from simulated long-slit data for the disk shown in Figure 3.

of Figure 3 show the rotation curves obtained with the slit oriented along the minor axis of the disk. The misalignment between the photometric and kinematic axes of the disk after 7.0 Gyr is clearly evident.

We have calculated the distribution of γ values for rotation curves obtained by observing the simulated disk at time $t = 7.0$ Gyr from 1000 random lines-of-sight with inclination angles limited to $30^\circ < i < 70^\circ$. A large fraction of rotation curves have values of γ significantly higher than the initial value of $\gamma = 1.3$. To be precise, approximately 45%, 25%, and 7%, have $\gamma > 2$, > 3 , and > 4 , respectively. Furthermore, minor axis rotation is seen with a peak amplitude exceeding 20% of the major axis amplitude in 70% of simulated rotation curves with $\gamma > 3$.

In Figure 4, we compare the high- γ LSB rotation curve shown in Figure 1 with one obtained from the projection

of the disk shown in Figure 3. The agreement between the simulated and observed rotation curves is excellent, suggesting that deviations from spherical symmetry in CDM halos might reconcile disk rotation curves that appear to favour the presence of constant density cores with cusps in the dark matter density profiles.

3. DISCUSSION

Given that we are able to match discrepant rotation curve shapes with a disk embedded in a cuspy triaxial halo, the outlook for reconciling dark matter cusps with LSB rotation curves is rather encouraging. However, it would be premature to argue that the problem has been fully solved. After all, given the number of extra “free” parameters introduced by relaxing the assumption of spherical symmetry, it is perhaps not surprising that one is able to improve the agreement with LSB rotation curves.

It is therefore important to build a more compelling case for this interpretation of LSB rotation curves, so as to render it falsifiable. Are there any corroborating traits that may be used to confirm or exclude the hypothesis that halos surrounding LSBs are indeed triaxial? In particular, we would like to understand better the particular combination of perspective and triaxiality that results in rotation curves with values of $\gamma > 1$. How can one best verify the triaxial-halo interpretation in two-dimensional velocity maps? Identifying a clean and unambiguous indication of triaxiality, such as the unusual minor axis kinematics shown in Figure 3, will be as important as the success of aspherical halos in reproducing the rich variety of shapes of LSB rotation curves. Only if this is accomplished shall we be able to conclude that LSB rotation curves do not preclude the presence of dark matter density cusps, thereby freeing the CDM paradigm of one vexing challenge on small scales.

This work has been supported by various grants to JFN from NSERC, CFI, and by fellowships from the Alexander von Humboldt Foundation.

REFERENCES

- Courteau, S. 1997, *AJ*, 114, 2402
 Davis, M., Efstathiou, G., Frenk, C. S., & White, S. D. M. 1985, *ApJ*, 292, 371
 de Blok, W. J. G., & Bosma, A. 2002, *A&A*, 385, 816
 de Blok, W. J. G., McGaugh, S. S., & Rubin, V. C. 2001, *AJ*, 122, 2396
 Flores, R. A., & Primack, J. R. 1994, *ApJ*, 427, L1
 Frenk, C. S., White, S. D. M., Davis, M., & Efstathiou, G. 1988, *ApJ*, 327, 507
 Fukushige, T., & Makino, J. 1997, *ApJ*, 477, L9
 —. 2001, *ApJ*, 557, 533
 Ghigna, S., Moore, B., Governato, F., Lake, G., Quinn, T., & Stadel, J. 2000, *ApJ*, 544, 616
 Hayashi, E., Navarro, J. F., Power, C., Jenkins, A., Frenk, C., White, S. D. M., Springel, V., Stadel, J., & Quinn, T. 2003, preprint [astro-ph/0310576]
 Jing, Y. P., Mo, H. J., Borner, G., & Fang, L. Z. 1995, *MNRAS*, 276, 417
 Jing, Y. P., & Suto, Y. 2002, *ApJ*, 574, 538
 McGaugh, S. S., & de Blok, W. J. G. 1998, *ApJ*, 499, 41
 Moore, B. 1994, *Nature*, 370, 629
 Moore, B., Governato, F., Quinn, T., Stadel, J., & Lake, G. 1998, *ApJ*, 499, L5
 Navarro, J. F., Hayashi, E., Power, C., Jenkins, A. R., Frenk, C. S., White, S. D. M., Springel, V., Stadel, J., & Quinn, T. R. 2004, *MNRAS*, 349, 1039
 Power, C., Navarro, J. F., Jenkins, A., Frenk, C. S., White, S. D. M., Springel, V., Stadel, J., & Quinn, T. 2003, *MNRAS*, 338, 14 (P03)
 Sellwood, J. A., & Kosowsky, A. 2001, in *ASP Conf. Ser. 240: Gas and Galaxy Evolution*, 311–+
 Spergel, D. N., & Steinhardt, P. J. 2000, *Physical Review Letters*, 84, 3760
 Swaters, R. A., Madore, B. F., & Trewhella, M. 2000, *ApJ*, 531, L107
 Swaters, R. A., Madore, B. F., van den Bosch, F. C., & Balcells, M. 2003, *ApJ*, 583, 732 (S03)
 Wadsley, J. W., Stadel, J., & Quinn, T. 2004, *New Astronomy*, 9, 137